Scientia Horticulturae 347 (2025) 114190

Contents lists available at ScienceDirect

Scientia Horticulturae

journal homepage: www.elsevier.com/locate/scihorti

Research Paper

Year and Flavescence dorée phytoplasma infection: impact on gene expression in two grapevine varieties

Marie-France Corio-Costet [a,*], Enora Bodin [a,b], Marie Laurens [a], Laure Dubois [b], Sylvie Malembic-Maher [b], Sandrine Eveillard [b,*]

[a] INRAE, Santé et Agroécologie du Vignoble, UMR 1065 33140, Villenave d'Ornon, France
[b] Univ. Bordeaux, INRAE, Biologie du Fruit et Pathologie, UMR 1332 33140, Villenave d'Ornon, France

ARTICLE INFO

Keywords:
Flavescence dorée phytoplasma
RT-qPCR
High-throughput gene expression
Molecular markers
Vitis vinifera
Vineyard

ABSTRACT

Flavescence dorée (FD) is a severe phytoplasma disease affecting grapevine (*Vitis vinifera*) in Europe, significantly impacting plant gene expression. This study aimed to (i) identify *in natura* gene expression differences between a highly susceptible cultivar (Cabernet Sauvignon) and a less susceptible one (Merlot), (ii) understand plant responses to FD phytoplasma (FDp) infection, and (iii) possibly identify molecular markers associated with lower susceptibility to FD. The expression of 95 grapevine genes was analysed by high-throughput RT-qPCR on symptomatic, non-symptomatic, and healthy branches collected in vineyards over two consecutive years.

Comparative analysis revealed cultivar-specific responses to FDp infection, year-specific expression patterns, and commonly modulated genes that could serve as markers of infection, health status, or varietal identity. Three genes were consistently down-regulated in Merlot compared to Cabernet Sauvignon, supporting the existence of varietal markers linked to genetic background. Several genes were specifically modulated in infected Merlot plants, including those related to defense and cell wall reinforcement, potentially contributing to restricted FDp movement. Non-symptomatic branches from infected vines showed intermediate expression profiles, suggesting systemic signaling or early responses.

These findings highlight the complex interaction between grapevine genotype, environmental conditions, and pathogen infection, providing a basis for identifying molecular markers and improving strategies to manage FD in vineyards.

1. Introduction

Phytoplasmas are wall-less plant pathogenic bacteria vectored by hemipteran sap-sucking insects of the Cicadellidae, Fulgoroidae and Psyllidae families (Trivellone and Dietrich, 2021). They are responsible for hundreds of diseases worldwide, leading to important economic losses (Bertaccini et al., 2014). Up to now, no curative treatments are available, and the only way to control the phytopathogen is to eliminate infected plants and apply insecticides against vectors. Phytoplasmas have small genomes that lack essential genes involved in amino acids and fatty acids biosynthesis or tricarboxylic acid cycle, among others. They have to acquire nutrients from their hosts, consequently modulating the host metabolism (Xue et al., 2018). They also have been shown to secrete effectors which diffuse in the plant and interact with transcription factors to modulate specific targets in their hosts, leading to changes in plant development but also influencing the insect vector behavior (Bai et al., 2009; Hoshi et al., 2009). Consequently, phytoplasmas are involved in many transcriptomic and metabolic changes in infected plants. Many studies reported the influence on the host gene expression, such as the expression of genes involved in primary (down-regulation in sugar and photosynthesis) and secondary metabolisms (up-regulation of PR protein genes and phenylpropanoid synthesis) in vines infected with '*Candidatus* Phytoplasma solani' responsible for Bois Noir disease (Hren et al., 2009a, 2009b). In sweet cherries infected with the sweet cherry virescence phytoplasma, glycolysis is modulated (Tan et al., 2021), or in vines infected with FDp, the JA/ET-mediated response, and the flavonoid metabolism are up-regulated (Bertazzon et al., 2019; Margaria et al., 2014; Pacifico et al., 2019). It is noteworthy that '*Ca.* P. solani' causes similar symptoms in grapevines as the FD phytoplasma (FDp) (Albertazzi et al., 2009; Hren et al., 2009a).

FD is a severe disease of grapevine in Europe. The associated agent is

* Corresponding authors.
E-mail addresses: marie-france.corio-costet@inrae.fr (M.-F. Corio-Costet), sandrine.eveillard@inrae.fr (S. Eveillard).

https://doi.org/10.1016/j.scienta.2025.114190
Received 25 September 2024; Received in revised form 22 April 2025; Accepted 14 May 2025
Available online 27 May 2025

the Flavescence Dorée phytoplasma (FDp) transmitted by the leafhopper *Scaphoideus titanus* Ball. (Schvester et al., 1963). FDp infection leads to serious damages like leaf discoloration, non-lignification of canes and grape wilting. Highly infected grapes did not even show any bunch, leading to important economic losses. As for other phytoplasma diseases, the use of insecticides against the vector is currently the only control measure available against FD along with the removal of the infected plants. Differences in susceptibility to FDp are observed in vineyards and under controlled conditions with, for example, Nebbiolo, Tocaï Friulano and Merlot (M) showing low FD susceptibility and Barbera, Chardonnay and Cabernet Sauvignon (CS) showing high susceptibility (Bertazzon et al., 2019; Casarin et al., 2023; Eveillard et al., 2016; Roggia et al., 2014). The poorly susceptible varieties show a low percentage of infected plants, low phytoplasma titers and a repressed diffusion of FDp (Casarin et al., 2023; Eveillard et al., 2016; Roggia et al., 2014). A genetic determinism of the susceptibility/resistance to FD is hypothesized as M and its mother, the Magdeleine Noire des Charentes, are both poorly susceptible, while CS and its parent Sauvignon are both highly susceptible (Eveillard et al., 2016). So, looking for grapevine varieties that are resistant or less susceptible to FD could be one complementary way to control FD, together with the measures already in place. Intensive analyses in infected vineyards could identify these varieties. Still, most of them are not present in infected areas or have not been planted yet if we refer to new varieties. FD inoculation under controlled conditions is an alternative. However, this procedure is time-consuming (Eveillard et al., 2016; Ripamonti et al., 2021). The identification of such varieties could be facilitated by using molecular markers of susceptibility when they become available.

From a transcriptomic point of view, FDp infection modulates the expression of genes involved in various pathways like sucrose and starch biosynthesis or defense, and it could even repress plant response to insect vector feeding in the susceptible Chardonnay (Bertazzon et al., 2019; Prezelj et al., 2016). Previous studies evidenced that molecular modulations differ between healthy and infected cultivars. They also suggested that these modulations could be associated with the cultivar susceptibility to FD (Bertazzon et al., 2019; Pacifico et al., 2019). We analysed the gene expression using a dedicated microarray to better understand the behavior of two varieties with contrasting susceptibilities in different health statuses (healthy or FDp-infected). The chip was used to identify markers of susceptibility or resistance directly in the vineyard at the end of the season for the two years under consideration. The results showed differentially expressed genes, allowing us to differentiate years, healthy/infected plant status and the two varieties.

2. Materials and methods

2.1. Observation and sampling in vineyard

The study site was located in Faleyras (44°77'1830"N, −0°22'6406"W) in the Bordeaux area, where two plots of M were grown alongside two plots of CS. The plants of the four plots were infected by the M54 FDp genetic variant, which is predominant in French vineyards (Malembic-Maher et al., 2020). The site was previously described in Adrakey et al. (2023) and is also presented in Figure S1. Plot C1 comprised 2259 CS, of which 665 were symptomatic in 2018, and C2 comprised 95 CS, of which 3 and 46 were symptomatic in 2018 and 2019, respectively. M1 comprised 677 M, of which 24 and 189 were symptomatic in 2018 and 2019, respectively, and M2 comprised 3025 M, of which 21 and 403 were symptomatic in 2018 and 2019, respectively. Mid-October 2018 and at the end of September 2019, the mappings of the symptomatic plants were performed, and symptom severity was noted. Plants were classified into four categories: <26 %, 26–50 %, 56–75 % and >75 % symptomatic branches on the plant as in Eveillard et al. (2016). A mean severity score value was calculated for each variety according to Adrakey et al. (2023). Following the observations, samplings were carried out in plots M1 and CS1 during 2018 and in plots M2 and CS2 during 2019 because CS1 was completely uprooted in compliance with FD management rules (proportion of infected plants higher than 20 %). Symptomatic plants of CS (35) and M (31) were selected randomly in the four categories of symptom severity (Table 1). Each sample was composed of ten petioles collected from a single plant, except for non-symptomatic samples, which were taken on a symptomatic plant that had already been sampled. Samples taken on an apparently symptomatic branch of infected vines were noted "-i" for "infected" (Fig. 1). All the samples were infected by FDp except for 2 M samples from 2018, which were not included. Samples taken on a non-symptomatic branch of an infected plant were noted "-ins" for "infected-non-symptomatic". FDp was also not detected in the non-symptomatic parts of infected plants (-ins), except in 1 CS-ins from 2018 to 2 from 2019, also not included in the study as they were exceptions. Samples were collected from 87 healthy plants (h) and 66 FDp-infected ones (i and ins) (Fig. 1). Samples from non-symptomatic FDp-uninfected vines were all negative for the presence of FDp except in 2 CS from 2019, which were not included in the analyses; subsequently, these samples will be considered as "healthy" for the rest of the article and noted "h" (CS-h, M-h). One cm sections of the petioles were immediately frozen in liquid nitrogen, and the rest was refrigerated at 4 °C. The numbers of samples in each severity category are detailed in Table 1.

2.2. DNA extraction

Nucleic acid extraction was carried out following a modified protocol based on the one described in (Maixner, 2005). In summary, 1 g of refrigerated petioles were ground in 6 ml cetyltrimethylammonium bromide (CTAB) buffer. One ml of the ground mixture was then used for the extraction. The final nucleic acids pellet was resuspended in 100 µl TE buffer (Tris 10 mM, ethylenediaminetetraacetic acid (EDTA) 1 mM pH 8). The nucleic acid concentration was determined using a BioTek™ Spectro Multi-Volume EPOCH spectrophotometer. The purity of the extract was evaluated by spectrophotometric measures of 260/280 nm and 260/230 nm ratios.

2.3. FDp detection and quantification

FDp cells were quantified as described in *Eveillard* et al. (2016). Two hundred ng of nucleic acids were used in the RT-qPCR experiment, and absolute quantification was done using a standard range of a plasmid carrying a fragment of the FDp *tuf* gene (Eveillard et al., 2016). FDp cells quantification was carried out using the LightCycler® 480 software release 1.5.0 (Roche), which automatically calculates the number of *tuf* gene copies in each tube by comparison with the standard range

Table 1
Number of samples analysed for Cabernet Sauvignon (CS) and Merlot (M) in plants with different sanitary status.

Variety	Year	Healthy (-h)	Infected non symptomatic (-ins)	Infected (-i)
Cabernet Sauvignon	**2018**	**20**	**7**	**14**
	2019	**19**	**19**	**21**
Merlot	**2018**	**24**	**11**	**9**
	2019	**24**	**20**	**22**

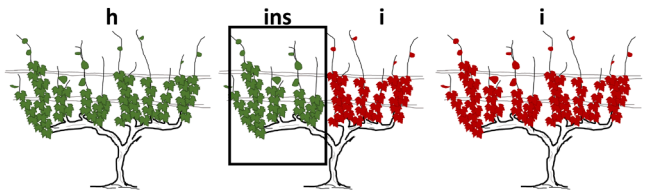

Fig. 1. Type of samples: "h" for healthy, "i" for infected with symptoms, and "ins" for infected non-symptomatic.

(Eveillard et al., 2016). The standard plasmid range was from 10E+1 to 10E+8 plasmids per well.

Specific detection of '*Ca.* P. solani' (*Stol11* genomic fragment) was done using a STOL11f2/r1 primer pair (Daire et al., 1997) followed by a nested PCR reaction with STOL11f3/r2 (Clair et al., 2003).

2.4. RNA extraction and gene expression analysis by RT-QPCR

Two ml of 56 °C preheated buffer (300 mM Tris–HCl, pH 8.0, 25 mM EDTA, 2 mM NaCl, 2 % CTAB, 2 % poly-vinyl poly-pyrrolidone (PVPP), 0.05 % spermidine trihydrochloride and 1 % β-mercaptoethanol) were added to 100 mg of plant petiole powder ground in liquid nitrogen and stirred vigorously, then incubated at 56 °C for 10 min as described previously (Bellée et al., 2018). After chloroform: isoamyl alcohol (24:1, v/v) extraction, we used the MagMAX™−96 Total RNA Isolation Kit protocol (Fisher scientific) for RNA purification: RNA was captured onto a binding bead using a unique binding solution, and genomic DNA was removed by DNase treatment according to the manufacturer's procedure. Purified RNAs were eluted in RNase-free water and stored at −80 °C. Fifty µl were then reverse-transcribed using RT-qPCR 100 µM oligo-d (T), ribonuclease inhibitor, and M-MLV reverse transcriptase (Promega, France) according to the manufacturer's instructions in a final volume of 110 µl. The cDNAs were then stored at −20 °C. Prior to their quantification, genes were amplified as follows: 1.3 µl of cDNA diluted to ~5 ng μl^{-1} and 3.7 µl of the reaction mixture containing 95 pairs of primers (primers pool, 50 mM), the PreAmp Master Mix (Standard Biotools) and DNA-free water were mixed. Fourteen amplification cycles were carried out, comprising 95 °C for 15 s and 60 °C for 4 min. Gene expressions were quantified using microfluidic dynamic array (Fluidigm) technology, with 95 primer sets of the « NeoViGen96 » and « Biostim » chips that were designed previously (Bodin et al., 2020; Dufour et al., 2016). The genes were selected to evaluate the plant's defence status and primary metabolism. Details of genes are listed in Table S1. Three grapevine genes (*VvEF1γ, VvTHIORYLS8, VvTIP41*) were used as references to normalize the cDNA template. A total of 95 primer pairs were tested. Seventy-two were analysed for the 2018 samples and 88 for the 2019 samples.

2.5. Data analysis

Q-PCR analysis with Fluidigm technology, data processing and statistical analyses were performed with R (R Core Team 2020) using the R Studio GUI (3.6.2 version). Data were subjected to an analysis of variance (ANOVA), and means were separated by Tukey's test ($p < 0.05$). Relative gene expression was considered differentially expressed for a p-value ≤ 0.05 in rank-bases non-parametric multiple comparisons, as described previously (Bodin et al., 2020). For FDp titers, statistical analyses were carried out with the Kruskal test using Rcmdr (Fox, 2005). To compare the gene expression of all modalities, CS-h-2018 was taken as a unique reference. In order to evaluate the effect of the year on the two healthy grape varieties, the gene expression data from the petioles of CS-h-18 and M-h-2018 were used as references for calculating the gene expression of CS-h-2019 and M-h-2019, respectively.

3. Results

3.1. Symptom severity and FDp titers in CS and M

As previously reported by Adrakey et al. (2023), the percentage of symptomatic vines was lower in Merlot (M) than in Cabernet Sauvignon (CS) in both 2018 and 2019 (see Materials and Methods and Figure S1), confirming a varietal effect. The mean symptom severity score across all plots and both years was 1.42 for M and 2.01 for CS. A year effect was also observed, with a slight overall decrease in symptom severity in 2019 across both varieties (1.98 in 2018 vs. 1.52 in 2019). Regarding phytoplasma load, the average FDp titers in M-i samples in 2018 and 2019 were 1.21E+06 and 4.82E+05 phytoplasmas/g fresh weight (fw), respectively (Fig. 2). In contrast, average FDp titers in CS-i in 2018 and 2019 were 8.51E+07 and 1.05E+07 phytoplasmas/gfw, respectively. The statistical analyses confirmed that FDp titers were consistently and significantly higher in CS-i than in M-i, in agreement with previous observations, as there were 70 and 22 times more FDp detected in CS-i than in M-i in 2018 and 2019, respectively. Additionally, FDp titers were lower in 2019 than in 2018 for both varieties, with a 2.5-fold decrease in M-i and an 8-fold decrease in CS-i.

3.2. Comparison of two grapevine varieties infected or uninfected with FDp: global features of the gene expression

Four contiguous plots in a vineyard experiencing an FD disease outbreak over two consecutive years were considered. For the study, petioles were sampled from healthy vines (CS-h, M-h), symptomatic branches of infected vines (CS-i, M-i), and non-symptomatic branches of infected vines (CS-ins, M-ins) over two years. Principal component analysis (PCA) revealed variations in gene expression based on the year of sampling, environmental conditions and infection status (Fig. 3). M and CS also showed different gene expressions in 2018 and 2019.

Regardless of their health status, the results showed that global genetic modulation was more pronounced in 2019 than in 2018 (Fig. 4), with some genes specifically expressed in the Merlot variety. This suggested a significant yearly effect, and revealed dynamic and varietal-specific responses to FD infection in grapevines.

3.3. Focus on healthy grapevine

3.3.1. Year effect

The year effect was perceptible in healthy plants (Figs. 3,4, S2-S3). In healthy CS (CS-h), most of the analysed genes were up-regulated (41 up-regulated/14 down-regulated) in 2019 compared to 2018. The pattern was more balanced in healthy Merlot (M-h), with 28 genes up-regulated and 23 genes down-regulated in 2019 compared to 2018 (Figures S2-

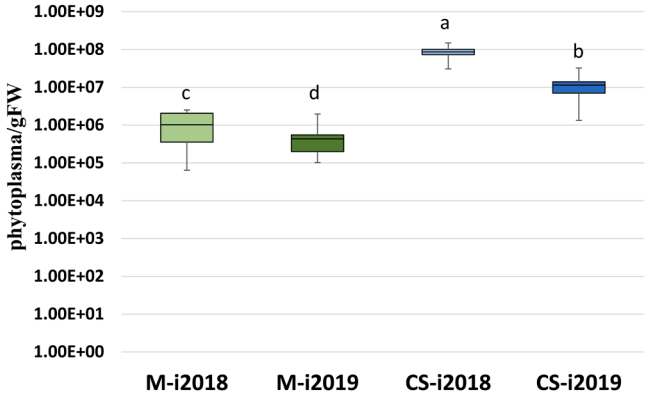

Fig. 2. Phytoplasma titers in CS and M in 2018 and 2019. M = Merlot, CS = Cabernet Sauvignon, h: healthy; ins: Infected non-symptomatic; i: infected. Statistical analysis: Kruskal with Rcmdr.

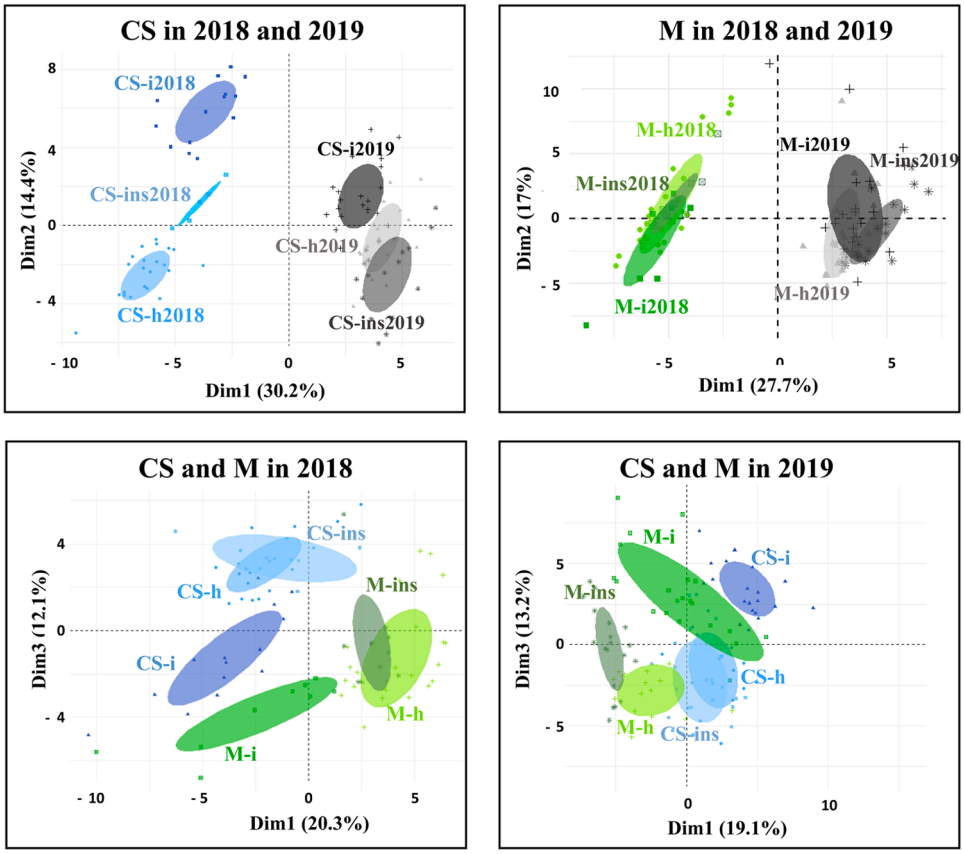

Fig. 3. Principal component analysis (PCA) of gene expression in Cabernet Sauvignon (CS) and in Merlot (M) in healthy plants (CS-h, M-h), infected symptomatic plants (CS-i, M-i) and infected non-symptomatic plants (CS-ins, M-ins), in 2018 and 2019 in the vineyard.

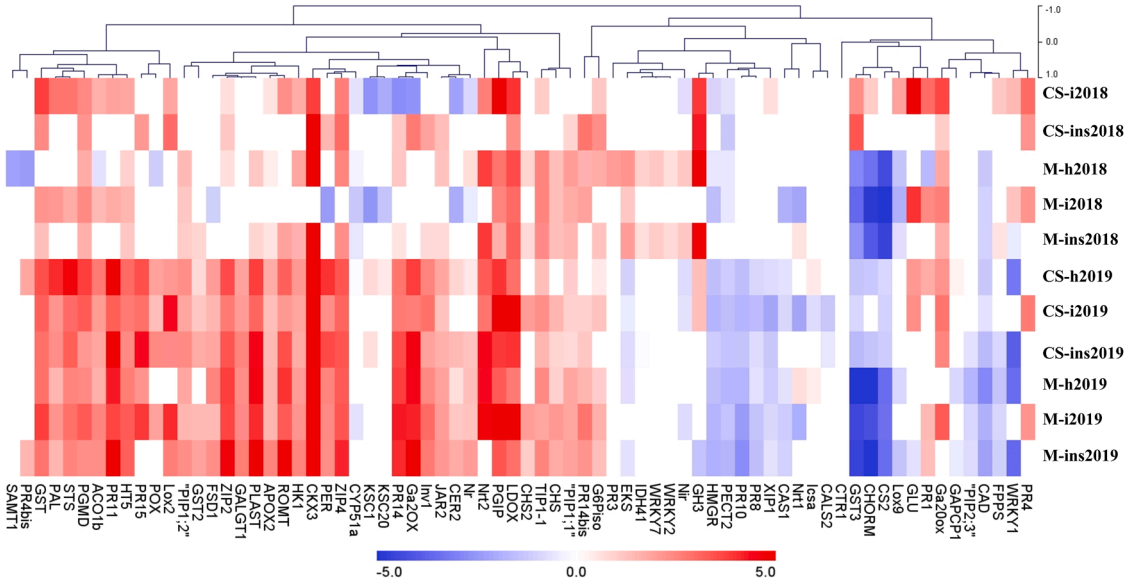

Fig. 4. Hierarchical clustering of gene expressions in CS and M, healthy (h), infected (i) or infected non-symptomatic (ins), in 2018 and 2019, relative to CS-h 2018. Each column corresponds to a modality (grape variety, year, health status), and each row corresponds to a gene. Color intensity is correlated with levels of expression; red for up-regulated genes and blue down-regulated ones. Expression data is reported in log2.

S3). Notably, 24 up-regulated and 12 down-regulated genes in year 2 *versus* year 1 were common to both CS and M plants (Figure S2). Among these commonly up-regulated genes (2019), a diverse array of pathways was represented, including defense (*e.g.* PR proteins *VvPR1, VvPR4b, VvPR1*), phenylpropanoid pathway (*e.g. VvPAL, VvSTS VvROMT*), oxidative stress response (*e.g. VvAPOX, VvFSD1*), cuticle formation (*e.g. VvCER2*), isochorismate pathway (*VvICS*), hormonal pathways (*e.g. VvGA2ox*), primary metabolism, and zinc homeostasis (*e.g. VvHT5, VvINV, VvPlast, VvNr, VvZIP-2,*) (Figs. 4, S2-S3). Additionally, genes down-regulated in both healthy grape varieties in 2019 were implicated

in defense mechanisms and isoprenoid pathways (*e.g. VvHMGR, VvEKS, VvCAS*), parietal structure biosynthesis (*e.g. VvCAD*), and aquaporins (*e.g. VvXIP1, VvPip2.3*), alongside nitrite reductase and chorismate mutase genes (*VvNiR* and *VvCHORM*).

These findings suggest that in 2019, even if no specific symptoms were visible, vineyard plants were likely subjected to various biotic or abiotic stressors, accounting for the heightened modulation of numerous genes involved in defense and stress responses. The observed modulation of genes between 2018 and 2019 was not limited to healthy grapevines but extends to infected ones. This suggests a significant influence of environmental factors, regardless of the grapevine variety.

3.3.2. *Varietal effect*

Transcriptomic disparities between CS and M were evident even in the healthy state, highlighting fundamental differences between these two varieties (Figure S2). When comparing both varieties, more genes were up-regulated in CS than in M in 2019. In healthy M, 16 genes were expressed in the same way in both years. Other genes followed similar expression patterns (Fig. 5A-B), while 17 genes were inversely modulated depending on the year (Fig. 5C-D). Furthermore, some genes consistently maintained similar expression patterns over the two years, either with similar intensities (Fig. 5A) or with some of them highly down-regulated (*VvCHORM, VvGST3, VvCS2*). We looked at the correlation between these 3 genes in the two grapevine varieties and according to their health status. Correlations between the three genes for the two years showed similar R^2 in CS and M healthy (R^2=0.72 and 0.75). On the other hand, in infected plants, the three genes were more correlated in CS than in M (R^2 = 0.84 in CS-i and 0.57 in M-i).

Overall, there were up-regulation of genes involved in the flavonoid pathway (*VvCHS*), nitrogen metabolism (*VvNr*), carbon metabolism

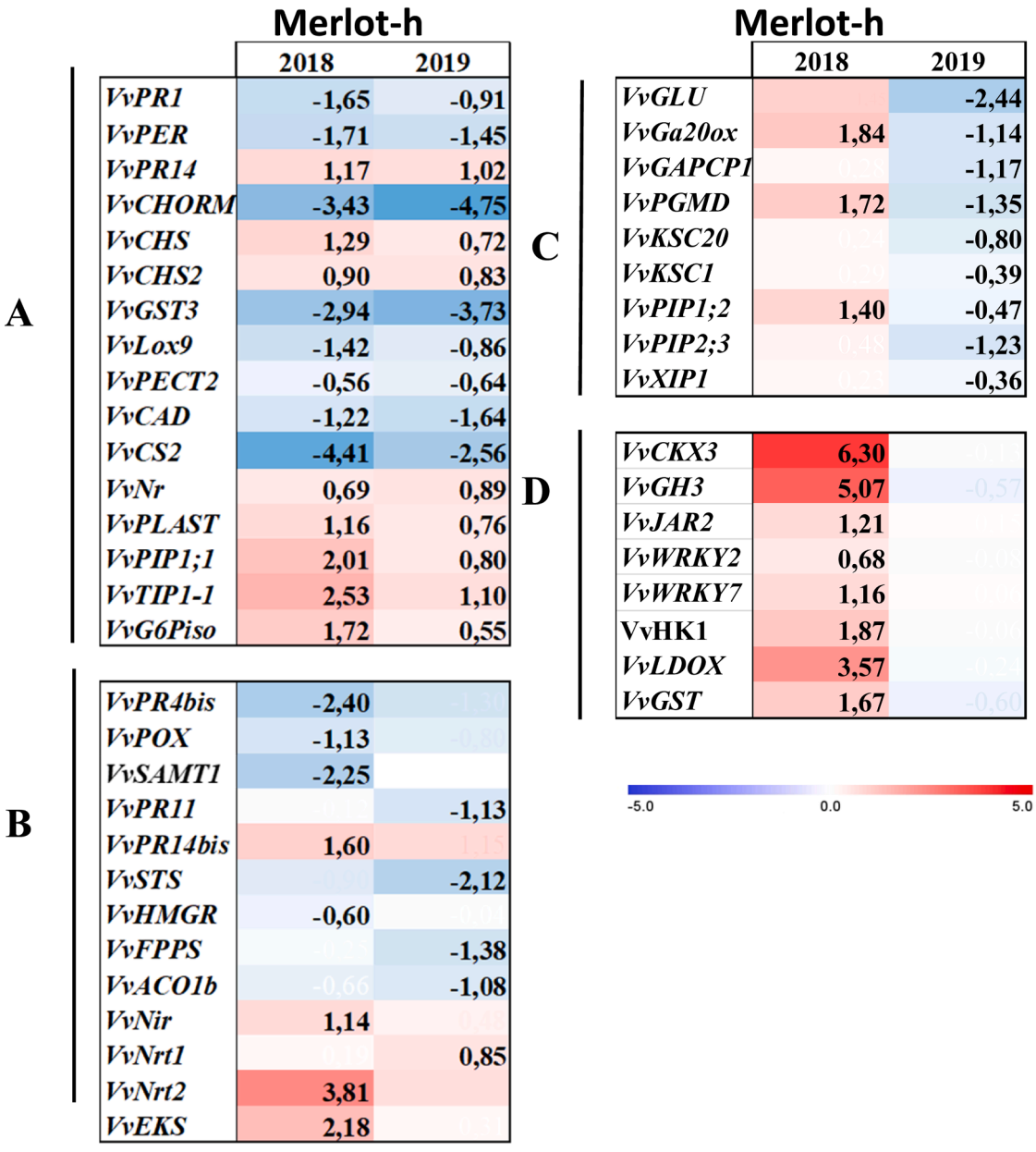

Fig. 5. Heatmap of relative expression (RE) of modulated genes (Fold change convert in log2) in healthy M relative to healthy CS in 2018 and 2019. The different boxes represent the common gene modulation, the two years (**A**), significant modulations only in 2018 or 2019 with the same trend (**B**), overexpression specific to 2018 and trend to antinomic modulations (**C-D**). The color scale is indicative of gene expression, up-regulated genes are shown in shades of red (log2(RE) > 0), with expression level higher than 5 in bright red, while down-regulated genes are in shades of blue (log2(RE) < 0), with intensity lower than −5 in dark blue. The numbers enclosed in boxes denote statistically significant gene modulation (Dunnett test, $p < 0.05$).

(*VvPlast, VvG6Piso),* aquaporins *(VvPIP1.1; VvTIP1.1)* and a lipid transfer protein (*VvPR14*). In contrast, genes involved in cell wall biosynthesis (*VvCAD, VvPECT*), PR proteins (*VvPR1* and *VvPER*) and oxilipin (*VvLox9*) were down-regulated. Some genes exhibited similar expression trends, albeit with varying intensities (Fig. 5B), and other gene groups appear to be more indicative of the year effect (Fig. 5C-D).

Overall, substantial distinctions between the two grape varieties, CS and M, were noticeable, highlighting the genetic background disparities between CS and M. Furthermore, some genes maintained consistent expression patterns across the two years, while others appeared to be influenced by year-specific factors. The constitutive differences could enable us to understand how CS and M respond to environmental variation (climate, pathogens) and highlight the complex interaction of genetics and environmental effects on grapevine health and disease.

3.4. Effect of FD phytoplasma infection on gene expression in CS and M

3.4.1. Global differences

The Venn diagrams (Fig. 6A) summarized the number of genes commonly or differentially modulated across different health states and/or varieties both in 2018 and 2019. In the case of infected plants, whether exhibiting symptoms ("-i") or not ("-ins"), we observed the year effect (greater gene modulation) similarly to what was observed in healthy plants (Fig. 6B). Notably, differences were observed between the two varieties. M presented fewer gene modulations than CS. This trend was consistent across the years, except for M-ins and CS-ins. In 2018, genes from CS petioles were predominantly up-regulated, whereas the prevalence of M petioles genes was down-regulated (Figs. 6, S4). However, in 2019, this pattern was reversed, underscoring the profound influence of year on gene expression in vineyards. Moreover, it was worth noting that samples collected from the non-symptomatic branches (-ins) of infected vines also displayed gene expression modulations, with fewer up- or down-regulated genes observed as compared to infected samples. These results underscored the notion that, even in the absence of apparent symptoms or detectable phytoplasma presence, molecular responses were triggered in grapevine -ins samples, with part of the response being shared with those observed in the symptomatic branches of infected plants (-i).

In summary, these findings highlight the substantial impact of infection on gene expression in both CS and M varieties, regardless of symptom presence.

3.4.2. Effect of FD on CS gene expression

As previously described, varying gene expression patterns of infected petioles were observed, probably linked to the year effect (Figs. 4, 6, S4). In 2018, 33 up-regulated and 11 down-regulated genes were observed in CS-i compared to CS-h, whereas in 2019, there were 20 up-regulated and 30 down-regulated genes (Figs. 6, S4, Table S2A). Up-regulated genes were associated with most pathways. Conversely, most down-regulated genes were related to nitrogen metabolism, cuticle formation, and parietal structure (Fig. 6, Table S2A). While the modulated pathways remained similar over the two years (Table S2), the specific genes involved often differed. However, some genes were consistently modulated, with the majority of them being up-regulated and linked to defense (*VvCHORM, VvLDOX, VvPGIP, VvPR4, VvLox9, VvLox2, VvWRKY1, VvTIP1–1, VvGST3*). At the same time, those down-regulated were primarily associated with primary metabolism *(VvNr, VvKSC1, VvCER2, VvKSC20, VvPECT2, VvCYP51, VvGA2ox*) (Fig. 6B, Table S2A).

In non-symptomatic petioles (CS-ins), most of the up-regulated genes in 2018 had similar patterns as CS-i (Fig. 6B, Table S2A). The shared genes were associated with various pathways, including flavonoid biosynthesis (*VvLDOX*), the jasmonate pathway (*VvLox2*), zinc transport, (*VvZIP*) carbon metabolism (*VvG6Piso, VvPGMD*), and defense (*VvGST 1, 3, VvPR4*). In the second year (2019), the trend shifted, with most genes being down-regulated, except for the flavonoid pathway (*VvCHS*) and *VvGST2*. This repression affected the ethylene pathway, the phenylpropanoid pathway (specifically stilbene biosynthesis), as well as genes involved in cell wall/cuticle formation and transport (aquaporin genes) (Figure 6B; Table S2A).

Notably, only two genes, *VvPR14* and *VvGA2ox*, exhibited a consistent gene modulation patterns in both years, specifically in CS-ins (Fig. 6B, Table S2A).

3.4.3. Effect of FD on merlot gene expression

As previously observed for CS, more genes were modulated in M-i in 2019 than in 2018 (Figs. 6, S4; Table S2B). In both years, genes

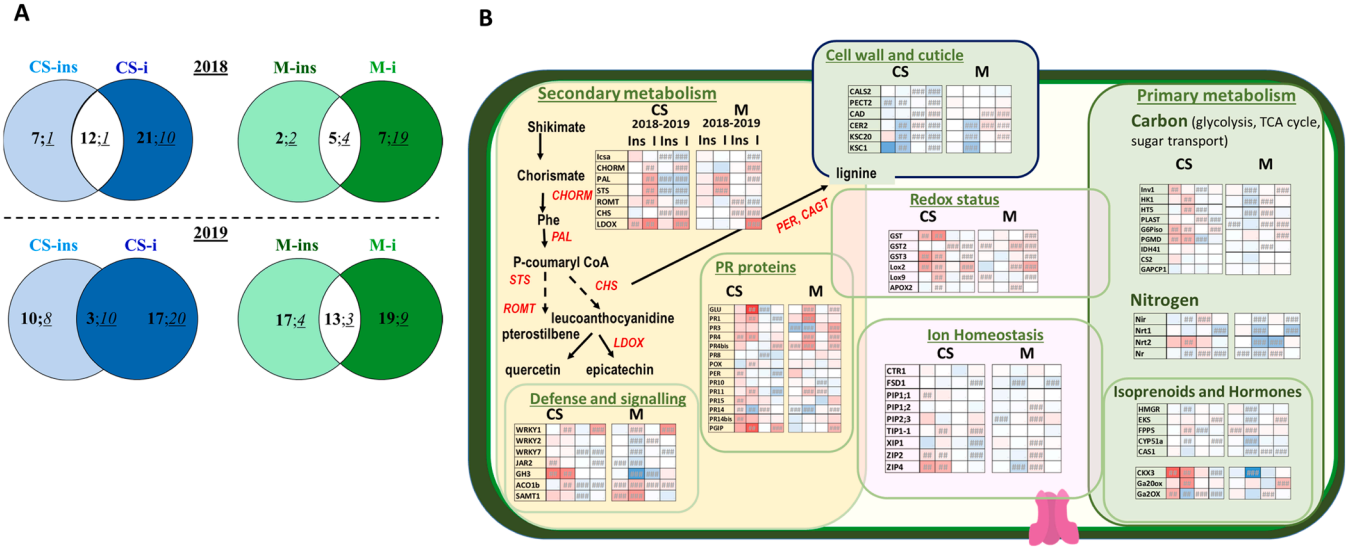

Fig. 6. (**A**) Venn diagram of differentially expressed genes in M and CS, infected with (i) or without symptoms (ins) in 2018 and 2019. Gene expression is relative to non-symptomatic plants for each variety and for each year. Bold: up-regulated gene; underlined italic: down-regulated genes. (**B**) Schematic representation of heatmap of relative expression (RE) of genes (log2) in infected and non-symptomatic plants for each variety (CS and M) relative to their respective controls (CS-h or M-h) for each year. The color scale is indicative of gene expression, with up-regulated genes in shades of red ($0 < \log2(RE) \leq 5$ in bright red) and down-regulated genes in shades of blue (-5 in dark blue $\leq \log2(RE) < 0$). The numbers enclosed in boxes denote statistically significant gene modulation (Dunnett test, $p < 0.05$).

associated with secondary metabolisms and expressed in infected grapevine were up-regulated. Specifically, *VvGST2* and genes belonging to the phenylpropanoid biosynthesis (*e.g., VvPAL),* PR proteins (*VvPR1, VvPR4*), signaling (*VvWRKY1*), and the ethylene pathways (*VvACO1b*) (Figs. 6B, S4; Table S2B). On the other hand, similarly to CS-i, down-regulated genes were mainly involved in primary metabolic pathways, including nitrogen metabolism (*VvNir, VvNrt1*), sterol biosynthesis (*VvCYP51, VvCAS*), transcription factor *VvWRKY7,* and a gene related to iron homeostasis (*VvFSD1).*

Regardless of the year, several pathways, primarily associated with defense mechanisms such as PR proteins and the phenylpropanoid pathway, exhibited similar regulatory patterns between M-i and M-ins. Nonetheless, only the *VvACO1b* gene, involved in the ethylene pathway, was commonly expressed between M-i and M-ins in both years. Intriguingly, genes from the carbon metabolism were up-regulated in both M-i and M-ins but only in 2019 (Figs. 6B, S4, Table S2-B). Additionally, genes related to structural components (*VvCER2, VvCAD*), those involved in the flavonoid pathway (*VvCHS, VvCHI*), and two genes from the ethylene and jasmonate pathways (*VvACOIb, VvLox2*) were also up-regulated in M-i and M-ins in 2019. In contrast, in 2018, three genes were up-regulated in M-ins and M-i in the hormonal pathway of ethylene and salicylic acid (*VvACO1b, VvSAMT1*), and one gene in the isoprenoid biosynthesis pathway (*VvFPPS*). In addition, two genes, *VvPR3* and *VvGH3* (endochitinase and jasmonate regulation), were consistently down-regulated in both M-i and M-ins in 2018.

To summarize, three genes were similarly modulated in symptomatic infected plants of both cultivars, regardless of the year and physiological state studied. Two of the genes, coding for a WRKY transcription factor (*VvWRKY1*) and a PR endochitinase (*VvPR4*), were up-regulated, while a gene involved in phytosterol biosynthesis, C14 demethylase (*VvCYP51*), was down-regulated. Looking deeper, we noticed a few trends in CS-i and M-i, with more pronounced repression of genes involved in cuticle formation (*VvCER, VvKSC1, VvKSC20*) in CS-i, in nitrate reductase and nitrogen transport (*VvNir, VvNrt1*), and superoxide dismutase (*VvFSD1*) in M-i (Fig. 6).

3.5. Comparison of gene expression in CS and M

3.5.1. Specific gene expression in M compared to CS, whatever the sanitary status

In both years, several gene expression patterns distinguished the M from the CS regardless of the sanitary status. Indeed, in 2018, M consistently exhibited significant up-regulation of four genes: chalcone synthase (*VvCHS)*, aquaporins (*VvPIP-1.2, VvPIP-1.1*), and gibberellin synthesis (*VvEKS*) genes, while five genes (*VvCAD, VvLOX9, VvCHORM, VvCS2, VvGST3*) were down-regulated, as mentioned above (cf.3.b). Three of these genes also demonstrated similar patterns in 2019, specifically associated with the M variety, namely, *VvCHORM, VvCS2* and *VvGST3*, suggesting their potential as varietal expression markers (in comparison to CS) (Figs. 4, 7A). Additionally, in 2019, *VvGAPCP1*, involved in the Calvin cycle, was notably down-regulated in M (Figure S6–1).

5.2. Comparison of gene expression in CS and in M infected plants (-i and -ins)

5.2.1. Gene expression in symptomatic plants (-i)

5.2.1.1. Common gene expression in CS-i and M-i. Symptomatic CS-i and M-i samples displayed unique gene expression profiles compared to healthy (-h) and non-symptomatic (-ins) samples. In both 2018 and 2019, there was a common up-regulation in both infected grape varieties of *VvWRKY1, VvPR4* and *VvLDOX,* along with down-regulation of the *VvCYP51* gene involved in the sterol metabolism and of the nitrogen pathway (*VvNrt1*) (Figs. 4, 7B). The FDp-infected plants, CS and M, modulated specific defense and nitrogen metabolism genes in response to phytoplasma presence in petioles. Therefore, our results suggest that the expression of these genes could potentially serve as a marker for FDp infection for these two cultivars, regardless of the year.

Some genes exhibited consistent expression patterns between the two grapevine varieties but not across years, highlighting differences among the years and suggesting a year-specific effect. In 2018, some

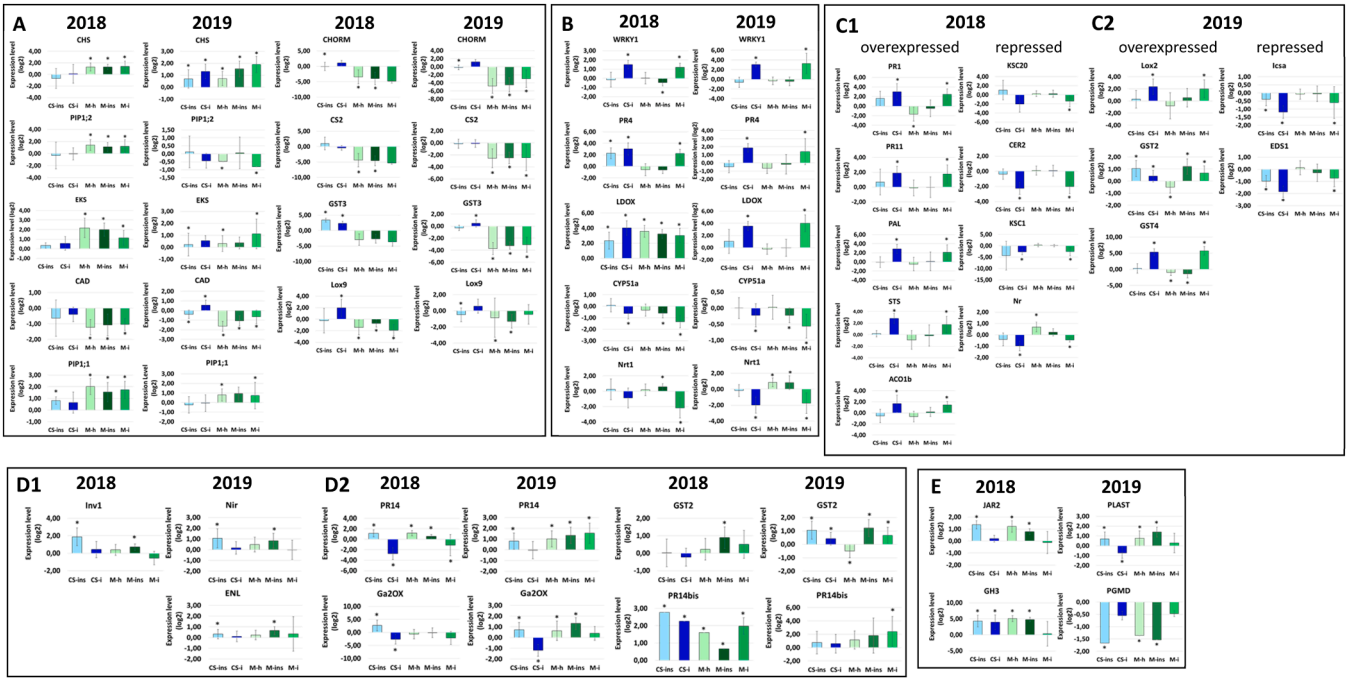

Fig. 7. Gene expression level (log2) in M and CS, healthy (-h), infected non-symptomatic (-ins) and infected (-i) relative to CS-h in 2018 or in 2019. **A**: genes differentially modulated between CS and M both years. **B**: genes commonly modulated in M-i and CS-i both years. **C:** genes commonly modulated in CS-i and M-i only in 2018 (C1) or 2019 (C2). **D**: genes commonly modulated in CS-ins and M-ins only in 2018 or 2019 (D1), and genes modulated both years in CS-ins or M-ins.

genes were up-regulated specifically in infected plants, but not in 2019 (*e.g. VvPR1, VvPR11, VvPAL, VvSTS, VvACO1b, VvNr*, Figs. 4, 7C; S6–2). Similarly, in 2019, genes involved in stress response (*VvGST2, VvLox2, VvGST4*) were up-regulated in both varieties, but not in 2018 (Figs. 7C, S6–2). Regarding down-regulated pathways in both grapevine varieties, some genes were repressed in 2018 but not in 2019 (*VvCER2, VvKSC20, VvKSC1*), while in 2019, the presence of FDp appears to lead to the repression of genes associated with defense and hormonal signaling (*VvICSa, VvEDS1*) (Figs. 7C, S6–2).

5.2.1.2. Differential gene expression in CS-i and M-i. In order to identify specific differences in the modulation of gene expression between CS-i and M-i, we compared M-i gene expression to CS-i gene expression of the relative year. Only genes previously identified as M markers regardless of the health status (*VvCHORM, VvCS2, VvGST3*) were differentially expressed over the two years (Figs. 7A, S5). It appeared, nonetheless, that specific genes, even though modulated in a similar way in M-i and CS-i according to the year (up-regulation of *VvGLU, VvPR4,* down-regulation of *VvCyp51,* Figure S4), displayed a much lower abundance of transcripts in M-i compared to CS-i (Figure S5) and could represent potential M-i specific modulations compared to CS-i. Conversely, others showed more abundant transcripts in M-i than in CS-i (*VvCHS, VvNr, VvPIP1.1*), corresponding to genes already specifically modulated in M-h during the two studied years (Fig. 7). Overall, the differences between M-i and CS-i were mainly related to the effect of the grape variety and the constitutive regulation of gene expression, which differed in M.

5.2.2. Specific gene expression in non-symptomatic infected plants (-ins)

Regarding the -ins status, no gene was commonly modulated for the two years in the two varieties. However, depending on the year, some primary metabolism genes were up-regulated in the two varieties, including *VvInv* in 2018 and *VvNir* and *VvEnl* in 2019 (Figs. 7D1, S6–3). In both years, the up-regulation of the *VvPR14* gene and *VvGa2ox* gene (involved in the catabolism of gibberellin) characterized CS-ins, while the up-regulation of *VvGST2* characterized M-ins (Fig. 7D2). It is worth noting that several genes were modulated identically in CS-ins, M-h and M-ins (*VvPR14, VvJAR2, VvGH3* in 2018 and *VvPLAST, VvPGMD* and *VvGa2ox* in 2019) (Figs. 7D2-E, S6–3). This observation may suggest that, similarly to M-h or M-ins, which are less susceptible to FDp infection, CS-ins could exhibit a comparable behavior—namely, a lower susceptibility to FD, as if in a "pre-defense phase." However, this state appears to be transient.

4. Discussion

We used high-throughput RT-qPCR with chips containing genes from the Neovigen and Biostim chips (Bodin et al., 2020; Dufour et al., 2016) to compare, *in natura*, at the end of the growing season, one highly susceptible to FD (CS) and one poorly susceptible (M) grapevine varieties. We looked at the differences considering their health status: uninfected non-symptomatic (noted healthy), infected and symptomatic branches and uninfected and non-symptomatic branches taken on an infected plant.

We confirmed that M limits phytoplasma multiplication and diffusion compared to what is already shown in Eveillard et al. (2016). The year effect on symptom severity and phytoplasma titers measured for both varieties may be attributed to the sampling, the climatic sequences and plant physiology, as well as responses to different biotic and/or abiotic stresses depending on the year considered. Indeed, the climate was different for the two years, with 2019 exhibiting a more intense thermal amplitude, a less rainy spring and a drier summer. A similar phenomenon was reported for Bois Noir (BN) infected vines in 2004 and 2005 (Hren et al., 2009a). However, in this case, symptom severity could also be attributed to the concentration of '*Ca.* P. solani' in the host and/or climatic differences (2004 was colder and wetter). Climate may explain the differences in phytoplasma titers as phytoplasma multiplication could be accelerated in plants under warmer conditions, as reported for '*Ca.* P. asteris' in chrysantemum (Galetto et al., 2011) and in faba bean with an optimum at 25 °C for FDp (Salar et al., 2013). The year effect also impacted gene expression, with a more intense modulation of genes belonging to all the tested pathways in 2019 (Fig. 6). Overall, the genes expressed in healthy CS or M were somewhat different in 2018 and 2019, illustrating the influence of the environment on plant development and the constitutive transcriptome of plants.

Various studies have examined the plant response to FD infection, in particular the transcriptome, generally late in the season when symptoms are visible (Albertazzi et al., 2009; Gambino et al., 2013; Margaria et al., 2014; Pacifico et al., 2019). They found that the highlighted regulation pathways (photosynthesis, PR-proteins, antioxidant responses) are common responses for different phytoplasma infections (*e.g.* FD or BN) (Bertazzon et al., 2019; Hren et al., 2009a, 2009b; Santi et al., 2013; Teixeira et al., 2020). In infected plants, we found that only three genes had a consistent expression pattern regardless of the variety or the year. These genes belonged to PR protein and stress responses (*VvPR4, VvWRKY1* –up-regulated and *VvCyp51* -down-regulated).

4.1. Difference between M and CS whatever the health status

Three genes, *VvCHORM* (phenylpropanoid pathway), *VvGST3* (oxido-reduction pathway) and *VvCS2* (tricarboxylic acid cycle, TCA), exhibited a strong down-regulation in M compared to CS, regardless of the year and health status, and represented expression markers for the Merlot compared to CS (Figs. 6–8). The first one, *VvCHORM* gene, encodes a chorismate mutase enzyme that converts chorismate to prephenate and leads to the synthesis of amino acids such as phenylalanine and tyrosine and reduced oxidative stress (ROS and lipid peroxidation). The second gene was a glutathione S-transferase gene (*VvGST3*) that is involved in the redox status of the plant, helping the plant to detoxify cells and eliminate ROS generated to control infection. Finally, the third Merlot marker gene was *VvCS2*, encoding for a citrate synthase that catalyzes the first step of the TCA cycle, a critical step in respiratory metabolism. This last repression suggested a different regulation of the citrate synthase and the TCA cycle in M. Since citrate synthase is an enzyme strongly regulated by the redox system, with implications for plant metabolism (Schmidtmann et al., 2014), we suggest that oxido-reduction activities were more regulated in M than in CS, through the down-regulation of the citrate synthase gene, but also the chorismate mutase gene (*VvCHORM*), the peroxidase (*VvPER*), glutathione peroxidase (*VvGST3*), cinnamoyl–CoA reductase (*VvCAD*), and *VvLOX9* (oxilipine) genes encoding proteins involved in oxido-reduction systems, whatever the year. All these genes were down-regulated in M compared with CS (Fig. 7).

The lower correlation observed for the three genes *VvCHORM, VvGST3*, and *VvCS2* in M-i compared to CS-i further suggests a differential modulation of the TCA cycle between the two varieties upon FDp infection. This may involve the accumulation of organic acids, as reported in '*Ca.* Phytoplasma aurantifolia'-infected citrus (Mollayi et al., 2015), as well as modulation of the stress response through the chorismate pathway and GST activity. Interestingly, these three genes were also down-regulated in M-i compared to CS-i in experiments where plants were under controlled conditions (Bodin et al., 2023). In addition to these three well-identified M marker genes, regardless of the health status and the year, we observed a down-regulation of the *VvPER* gene, an up-regulation of the chalcone synthase (*VvCHS*), the gibberellin pathway (*VvEKS*) (associated with repression of the *VvCyp51,* a phytosterol biosynthesis gene) and aquaporin gene (the tonoplastic aquaporin gene capable of transporting water and hydrogen peroxide (*VvTIP1.1*) and a plasmic membrane aquaporin capable of transporting CO2 and water (*VvPIP1.1*). Regarding the aquaporin genes (*VvPIP1.1* and *VvTIP1.1*), they were strongly up-regulated in the M variety in both

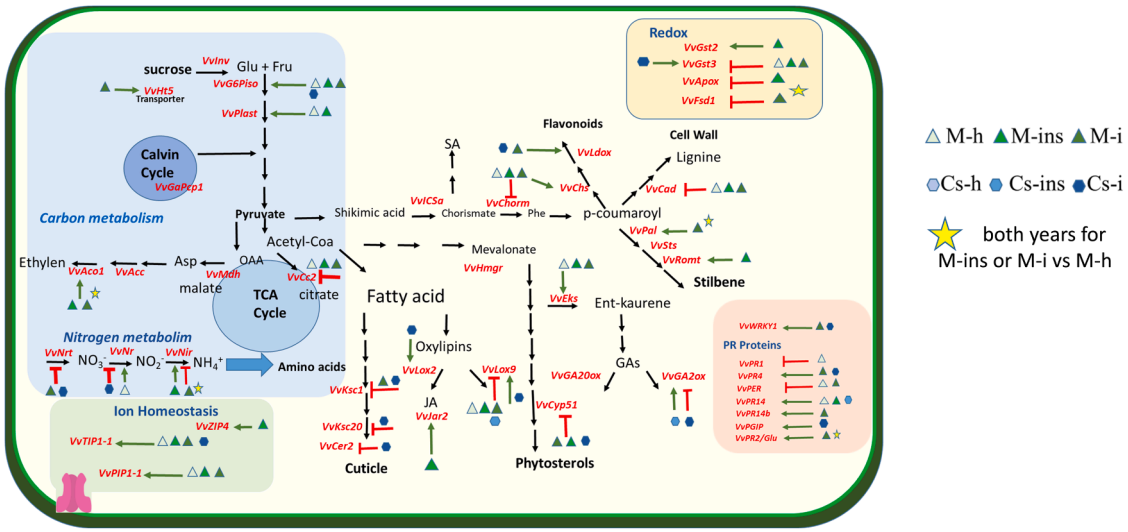

Fig. 8. Simplified diagram summing up the main effects of gene modulation for two consecutive years observed in M (green triangles) and CS (blue hexagons) infected or not. The green arrow symbolizes up-regulation, and the red arrow down-regulation relative to CS-h. The lightest color (green or blue) corresponds to healthy status, the medium color indicates non-symptomatic status, and the darkest color indicates symptomatic infected grape plants.

years, compared to the CS variety. M has smaller vessels than CS, so it is plausible that aquaporins (TIP and PIP), which are involved in the transport and water balance and other solutes, are up-regulated to offset (Pouzoulet et al., 2017). Aquaporins are implicated in the defense of sweet orange (*Citrus sinensis* L. Osbeck) against '*Ca.* Liberibacter asiaticus', a phytopathogenic bacterium also situated in the phloem (Martins et al., 2015). They could possibly be involved in the lower susceptibility of M.

The different modulation of expression of all these genes in M *versus* CS could be an indication that the reduced susceptibility of the M variety to FD could be related to the regulation of a gene network, including the three mentioned above, the oxidative stress regulation, the isoprenoid and the flavonoid pathway and aquaporins.

4.2. What are the differences in gene expression between healthy CS and M?

In addition to the genes mentioned above, healthy M could be characterized by a number of additional gene modulations (repression of *VvPR1*) or common to non-symptomatic M-ins, with the up-regulation of a gene involved in glycolysis (*VvPLAST*) and one coding for an aquaporin (*VvPIP1.1*) (Figs. 5, 8). These transcriptional differences reinforced the genetic disparities and constitutive differences between healthy CS and M.

In natura, healthy CS and healthy M were well differentiated by gene modulations involved in various defense and primary metabolism pathways. In agreement with Bertazzon et al., 2019, these gene modulations could be related to grapevine susceptibility to FD. In our work, the flavonoid pathway (*VvCHS*) was up-regulated in the poorly susceptible variety M as in Tocaï, which is scarcely susceptible too (Bertazzon et al., 2019).

The Lipid transfert proteins (LTP) are described as antimicrobial proteins (Amador et al., 2021), and as reported above, *VvPR14* (LTP) was up-regulated in M-h in both years. In contrast, *VvCAD* and *VvPECT2* were significantly down-regulated in M-h in both years and even in infected petioles compared to CS-h. We suggested that this possible limitation of the lignin pathway, compared to CS, could favour the accumulation of higher amounts of flavonol glycosides (Thévenin et al., 2011), with a redirection towards the phenolic pathway that can potentially limit the development of FD (Fig. 8).

Overall, carbon and nitrogen metabolisms tended to be more up-regulated in M-h than in CS-h, with up-regulation of genes coding for nitrate reductase (*VvNr*) or nitrogen transport (*VvNrt*) for the first glycolysis enzyme (*VvG6Piso*), and *VvPLAST*, a chloroplastic aldolase capable of increasing photosynthesis and playing a role in stress responses and growth (Lu et al., 2012).

The apparently healthy branch samples collected from symptomatic grapevines exhibited an expression pattern only partially similar to that of healthy samples. This suggests that the phytoplasma, although not yet detected in these samples, may in some cases influence the plant's transcriptome. We did not identify any marker gene consistently associated with this condition across both years. However, it is worth noting that in both years, CS-ins samples showed modulation of specific genes—such as *VvPR14*—that was similar to that observed in M-h. Specifically, for *VvPR14*, CS-ins differed from CS-h, indicating a response to a signal likely originating from the infected part of the plant and resembling the expression profile of M-h. This observation could be related to the reduced susceptibility of M to FD, which, in the healthy state, appears to behave similarly to an -ins condition.

4.3. Effect of FDp-infection on gene expression in both cultivars

4.3.1. Common up-regulated genes

Genes specifically up-regulated in both CS-i and M-i, as previously mentioned, were *VvWRKY1* (transcription factor) and *VvPR4* (PR protein endochitinase) involved in defense, and confirmed as a marker of FD infection (Figs. 6–8). Concerning the WRKY1 factor, in a study conducted over several years, Hren et al. (2009a) report that a WRKY factor is also up-regulated in grapevine Chardonnay infected with '*Ca.* P. solani'. This overexpression of the *VvWRKY1* gene associated with the SA pathway in defense has been described by several authors in '*Ca.* P. solani'-infected plants (Albertazzi et al., 2009; Dermastia, 2019; Gambino et al., 2013; Hren et al., 2009a). Also, significant expressions of a number of *VvPR* genes (*VvPR1, VvPR2, VvPR4, VvPR5* and *VvPR10*) involved in plant defense, were in agreement with the results of Casarin et al. (2023) in the poorly susceptible variety Tocaï Friulano. Some of them were also described in FDp-infected grapevines in other cultivars like Barbera and Nebbiolo (Gambino et al., 2013; Margaria and Palmano, 2011), along with an accumulation of SA in the veins (Prezelj et al., 2016). Note that we found some gene modulations in common with the study of Dermastia et al. (2021) on the Zweigelt grape variety for *VvPR10, VvPR1* and *VvAPOX*.

Other genes involved in phenylpropanoid pathway were up-regulated in the FDp-infected varieties like *VvLDOX* and *VvCHS* of the

flavonoid pathway, which were up-regulated in both years, suggesting a possible higher synthesis of flavonoids like leucoanthocyanidin and derivatives (*e.g.* anthocyanin, catechin and quercetin derivatives). This is in agreement with phytoplasma effect in Pinot gris and Sangiovese leaves, respectively (Davosir et al., 2023; Negro et al., 2020), or in FD-infected Nebbiolo and Barbera grape varieties, where flavonoid pathway genes were more up-regulated than in healthy plants (Margaria et al., 2014). With regard to stilbenes, the phenyl ammonia lyase gene (*VvPAL*) was up-regulated in CS-i and M-i, according to studies describing PAL up-regulation after phytoplasma infection (Hren et al., 2009a; Kaviani et al., 2022).

In general, genes of the carbon metabolism (sugar transport, invertase, glycolysis) were positively modulated in petioles of infected varieties, especially in 2018, with a higher and more significant intensity in M. This is in agreement with the effects of infection of phytoplasmas on the overexpression of sucrose synthase after '*Ca.* P. solani'-infection (Hren et al., 2009b; Margaria et al., 2014) and on glycolysis (Tan et al., 2021). All this suggested that the phytoplasma could reprogram the plant's metabolism to obtain the energy and nutrients it needs (Bertazzon et al., 2019; Hren et al., 2009b; Teixeira et al., 2020; Wei et al., 2013).

We confirmed that FDp-infection induced grapevine defense genes (PR protein, WRKY factor, genes involved in the flavonoid pathway and in antioxidant activities (*VvFSD, VvGST, VvAPOX*, etc.), with variations linked to the grapevine variety, as described by numerous authors (Bertazzon et al., 2019; Gambino et al., 2013; Margaria et al., 2014).

4.3.2. Common down-regulated genes

Concerning cell wall and cuticle, Qiao et al. (2023) have reported higher production of cutin, suberin and waxes after infection in *Camptotheca acuminata* infected with the *C. acuminata* Witches'-broom phytoplasma (CaWB, ribosomal group 16SrXXXII) with up-regulation of *KSC1* coding for ketothiolase. In our study, *VvKSC*1 and *VvKSC*20 were down-regulated in CS-i and M-i, still to a greater extent in CS-i than in M-i, suggesting a disruption in the cuticle pathway. This would indicate the cuticle's likely role in the response to phytoplasma infection, and the differences in symptomatology between FD and CaWB may explain the opposite results.

In FDp-infected grapevines, *VvCAD* and *VvPECT* genes were rather down-regulated in symptomatic plants, mainly in M-i. This modulation could be related to a potential shift towards stilbenes and flavonoids (Fig. 8). By comparison, in non-symptomatic Tocaï friulano, Bertazzon's transcriptomic analysis at an early time point reported activation of the cinnamoyl-CoA reductase gene (*VvCAD*) and repression of the pectin methylesterase gene (*VvPECT*), both involved in cell wall structure. In contrast, M-i and CS-i showed opposite regulation of these genes, with a down-regulation of the lignin pathway in favour of the phenylpropanoid pathway in infected plants. This difference in gene modulation may be explained by differences in symptom expression and sampling time between the two studies, as M-i and CS-i samples were symptomatic, whereas Tocaï friulano samples were not.

Teixeira et al. (2020) described that FD generally represses the isoprenoid pathway (carotenoid, quinones, tocopherol, etc.) in the grapevine Loureiro. In agreement, the isoprenoid pathway appeared here to be affected by FD in both varieties CS and M the two years, with a repression of the gene encoding for C14 demethylase (*VvCYP51*), a key gene in phytosterol biosynthesis, and to a lesser extent the *VvHMGR* gene coding for protein located upstream in the isoprenoid pathway.

4.3.3. Modulation of the hormonal pathways-involved genes

Partially linked to the isoprenoid biosynthesis pathway, infection with FD phytoplasma leads to reprogramming of the host plant's metabolism, with marked changes in hormonal pathways (Dermastia, 2019). Here, the modulation of the gibberellin pathway (*VvEKS, VvGa2ox* and *VvGa20ox*) corroborated the one described by Nejat et al. (2015) and Mardi et al. (2015) for other phytoplasmas. The *VvACO1* involved in the ethylene pathway was up-regulated as described by Gambino et al. (2013) after FDp infection, and even more in M-i than in CS-i. This regulation is also supposed to be involved in the recovery state of the Barbera variety (Pacifico et al., 2019). The JA pathway (*VvLox2*) was also modulated (rather activated) in CS-i in both years but only in 2019 for M-i, confirming a potential role of the JA pathway in agreement with Bertazzon et al., 2019. Moreover, modulations of *VvJAR2* and *VvJAR1/GH3* genes, involved in JA regulation and even required for flavonoid accumulation (Miyamoto et al., 2016; Wasternack and Feussner, 2018) were observed, either up- or down-regulated in 2018 or in 2019, in both varieties, supporting the JA role after infection. Paolacci et al. (2017) reported repression of the salicylic acid (SA) pathway and overexpression of the jasmonic acid (JA) pathway in response to BN infection. In our study, over the course of two years, the expression of genes involved in SA methylation (*VvSAMT*), ethylene biosynthesis (*VvACO1*), and JA synthesis and regulation (*VvLOX2, VvJAR25, VvGH3*) varied between years in infected plants. These variations could be linked to differences in infection levels but also to responses to other abiotic and biotic stresses. It is likely that the SA, JA, and ethylene pathways interact through cross-talk mechanisms following infection. However, this interaction may occur at a level insufficient to trigger an effective defense response against FDp, as similarly observed in plants facing other pathogens or after defense stimulation (Nawaz et al., 2023).

4.3.4. Specific variation in M-i

As described above, three genes that differentiated CS and M whatever their health status, were reported: *VvGST3, VvCHORM* and *VvCS2*. In addition, some deregulations were specific of M-i, or at least were more intense in M-i than CS-i (Figs. 8, S5). Most of these genes mentioned in Figure S4 also had the same deregulation under controlled conditions (Bodin et al., 2023).

Concerning *VvPR14,* this LTP gene was significantly more up-regulated in both years in M-i than in CS-i. This LTP plays a role in resistance to biotic and abiotic stresses (Jülke and Ludwig-Müller, 2016; Laquitaine et al., 2006; Safi et al., 2015) and could play a role in the reduced susceptibility of M.

The *VvPIP1–1* transcripts, coding for an aquaporin gene, were also abundant in M-i, which could be related to the role of PIP1–1 in promoting the circulation between phloem and xylem vessels and the transport of sap in the plant (Kaldenhoff et al., 1998). The sap could then transport defense signals and sugar as energy molecules used for defense.

We noticed that the callose synthase gene (*VvCALS*) was up-regulated in M-i as compared to CS-i, in combination with the down-regulation of glucanase (*VvGLU*) known to degrade callose at plasmodesmata to facilitate transport. This suggests that callose could be a way to block the diffusion of the FDp in the plant. It could be more efficient in defense in M-I, especially when both genes *VvGLU* and *VvCALS* were modulated.

The ent-kaurene synthase gene (*VvEKS*), upstream of sterol biosynthesis and involved in gibberellin biosynthesis, was up-regulated in infected plants but more pronounced in the least susceptible variety (M), suggesting a reprogramming towards the isoprenoid pathway. This restriction of the final phytosterol pathway favouring the gibberellin pathway with ent-kauren, could be similar to maize which uses this pathway for the synthesis of kauralexin-type molecules with antibiotic activity when infected with *Fusarium* species, for example (Ding et al., 2019; Murphy et al., 2021).

In summary, M is thought to modulate certain metabolic pathways in a different way, including that of the phenylpropanoids, to the detriment of the lignins. In terms of PR protein-type defenses overall, the M variety up-regulated more PR proteins than CS, especially LTPs and strongly down-regulated the redox system genes compared to CS. Carbon metabolism (glycolysis and gluconeogenesis), nitrogen reductases and homeostasis genes (in particular aquaporins) appear to be more active in M (Fig. 8). Regarding hormones, the ethylene and gibberellin pathways

also appear to be positively modulated in infected Merlot. Our results suggest that JA-SA-Ethylene cross-talk are different between the two varieties, with CS involving more JA and M more AS.

All these gene modulations combined could indicate that M-i, in contrast to CS-i, exhibited less intensive modulations of oxidative stress and sterol biosynthesis, favoring parietal structure and primary metabolism and lipid transfer protein.

Concerning the -ins samples, interestingly, over the two years, results showed that genes from these samples sometimes behaved like those from a healthy plant and sometimes like those of a symptomatic one. This indicates that the non-symptomatic part of an infected plant that was otherwise symptomatic responded to the infection by modulating gene expression, even in the absence of phytoplasma. The most significant differences between the CS-ins and M-ins in both years were the up-regulation of *VvPR14* and *VvGa2ox* in CS-ins, and the up-regulation of *VvGST2* in M-ins. These results may indicate that up-regulation of these genes in the healthy part of infected plants plays an important role in a possible resilience.

5. Conclusion

The aim of this study was to investigate plant gene expression deregulations and identify the differences, if any, between a highly FD-susceptible grapevine variety and one that is less. We also tried to decipher the mechanisms underlying the grapevine response to FD phytoplasma infection under vineyard conditions for two consecutive years. Gene expression of CS and M varieties was analysed *in natura* by high-throughput qRT-PCR in two consecutive years, and significant differences were observed in terms of variety and health status, indicating that there was indeed a reprogramming.

Regardless of health status, we identified three genes that were consistently more strongly down-regulated in M compared to CS, supporting the hypothesis that varietal markers exist between these two grapevine cultivars, reflecting differences in their genetic background. Potential marker genes of FDp infection common to both CS and M were also identified. These include genes related to PR proteins and stress response, as well as the phenylpropanoid and isoprenoid pathways. Their involvement is expected, as these pathways are commonly associated with plant defense against biotic stress. In addition to the three varietal marker genes, several genes were specifically modulated in M-i, including Chalcone synthase, LDOX, Callose synthase, glucanase, and aquaporin genes. These differences may contribute to a stronger defense response in M, potentially leading to higher levels of defense-related molecules and a more effective restriction of FDp movement through the vascular system compared to CS.

Interestingly, the -ins samples sometimes resembled the healthy (-h) samples and other times the infected (-i) ones, which may be linked to the presence of mobile signal molecules. The most notable differences between CS-ins and M-ins across both years were the up-regulation of VvPR14 and VvGA2ox in CS-ins and VvGST2 in M-ins. These findings suggest that the induction of these genes in the apparently healthy parts of infected plants may play a role in resilience mechanisms. It would be worthwhile to test the identified putative varietal marker genes, as well as the potential marker genes of FDp infection in CS and M on a wide range of varieties and at different times of the growing season under different environmental conditions, in order to validate them.

Funding

This work was supported by the project Co-Act (program “Plan National Dépérissement du Vignoble”, FranceAgriMer/CNIV), INRAE, and the IdEX Bordeaux University “Investments for the Future” program GPR Bordeaux Plant Sciences.

CRediT authorship contribution statement

Marie-France Corio-Costet: Writing – review & editing, Writing – original draft, Supervision, Formal analysis, Data curation. **Enora Bodin:** Methodology, Data curation. **Marie Laurens:** Methodology, Data curation. **Laure Dubois:** Methodology. **Sylvie Malembic-Maher:** Writing – review & editing, Funding acquisition, Conceptualization. **Sandrine Eveillard:** Writing – review & editing, Writing – original draft, Supervision, Formal analysis, Data curation, Conceptualization.

Declaration of competing interest

The authors declare the following financial interests/personal relationships which may be considered as potential competing interests:

INRAE reports financial support was provided by French National Institute for Agriculture and Seafood Products. INRAE reports financial support was provided by National Committee of Wine Interprofessional Organizations with Designation of Origin and Geographical Indication. If there are other authors, they declare that they have no known competing financial interests or personal relationships that could have appeared to influence the work reported in this paper.

Acknowledgements

The authors thank the experimental team of UMR BFP and UMR SAVE (INRAE, Bordeaux, France) for providing materials, logistics and assistance during the experimentation, in particular C. Garcion, B. Batailler, T. Lusseau. We are grateful to B. Ducos and M. Delagrange from Ecole Normale Supérieure (ENS-Paris) for using the BiomarkTM HD system and B. Chouaia for copyediting the manuscript.

Supplementary materials

Supplementary material associated with this article can be found, in the online version, at doi:10.1016/j.scienta.2025.114190.

Data availability

Data will be made available on request.

References

Adrakey, H.K., Gibson, G.J., Eveillard, S., Malembic-Maher, S., Fabre, F., 2023. Bayesian inference for spatio-temporal stochastic transmission of plant disease in the presence of roguing: a case study to characterise the dispersal of flavescence dorée. PLoS Comput. Biol. 19, e1011399. https://doi.org/10.1371/journal.pcbi.1011399.

Albertazzi, G., Milc, J., Caffagni, A., Francia, E., Roncaglia, E., Ferrari, F., Tagliafico, E., Stefani, E., Pecchioni, N., 2009. Gene expression in grapevine cultivars in response to Bois Noir phytoplasma infection. Plant Sci. 176, 792–804. https://doi.org/10.1016/j.plantsci.2009.03.001.

Amador, V.C., Santos-Silva, C.A.D., Vilela, L.M.B., Oliveira-Lima, M., de Santana Rêgo, M., Roldan-Filho, R.S., Oliveira-Silva, R.L.de, Lemos, A.B., de Oliveira, W.D., Ferreira-Neto, J.R.C., Crovella, S., Benko-Iseppon, A.M., 2021. Lipid transfer proteins (LTPS)-structure, diversity and roles beyond antimicrobial activity. Antibiotics (Basel) 10, 1281. https://doi.org/10.3390/antibiotics10111281.

Bai, X., Correa, V.R., Toruño, T.Y., Ammar, E.-D., Kamoun, S., Hogenhout, S.A., 2009. AY-WB phytoplasma secretes a protein that targets plant cell nuclei. MPMI 22, 18–30. https://doi.org/10.1094/MPMI-22-1-0018.

Bellée, A., Cluzet, S., Dufour, M.-C., Mérillon, J.-M., Corio-Costet, M.-F., 2018. Comparison of the impact of two molecules on plant defense and on efficacy against *Botrytis cinerea* in the vineyard: a plant defense inducer (Benzothiadiazole) and a fungicide (Pyrimethanil). J. Agric. Food Chem. 66, 3338–3350. https://doi.org/10.1021/acs.jafc.7b05725.

Bertaccini, A., Duduk, B., Paltrinieri, S., Contaldo, N., 2014. Phytoplasmas and phytoplasma diseases: a severe threat to agriculture. Am. J. Plant Sci. 5, 1763–1788. https://doi.org/10.4236/ajps.2014.512191.

Bertazzon, N., Bagnaresi, P., Forte, V., Mazzucotelli, E., Filippin, L., Guerra, D., Zechini, A., Cattivelli, L., Angelini, E., 2019. Grapevine comparative early transcriptomic profiling suggests that flavescence dorée phytoplasma represses plant responses induced by vector feeding in susceptible varieties. BMC Genomics 20, 526. https://doi.org/10.1186/s12864-019-5908-6.

Bodin, E., Bellée, A., Dufour, M.-C., André, O., Corio-Costet, M.-F., 2020. Grapevine stimulation: a multidisciplinary approach to investigate the effects of biostimulants

and a plant defense stimulator. J. Agric. Food Chem. 68, 15085–15096. https://doi.org/10.1021/acs.jafc.0c05849.
Bodin, E., Jollard, C., Dassé, A., Dufour, M.-C., Razan, F., Desqué, D., Corio-Costet, M.-F., Malembic-Maher, S., Eveillard, S., 2023. Insights into grapevine gene responses to flavescence dorée. phytoplasma. Phytopathogenic Mollicutes 19–20.
Casarin, S., Vincenzi, S., Esposito, A., Filippin, L., Forte, V., Angelini, E., Bertazzon, N., 2023. A successful defence strategy in grapevine cultivar "Tocaï friulano" provides compartmentation of grapevine flavescence doree phytoplasma. BMC Plant Biol 23, 161. https://doi.org/10.1186/s12870-023-04122-0.
Clair, D., Larrue, J., Aubert, G., Gillet, J., Cloquemin, G., Boudon-Padieu, E., 2003. A multiplex nested-PCR assay for sensitive and simultaneous detection and direct identification of phytoplasma in the Elm yellows group and Stolbur group and its use in survey of grapevine yellows in France. Vitis 42, 151–157.
Daire, X., Clair, D., Reinert, W., Boudon-Padieu, E., 1997. Detection and differentiation of grapevine yellows phytoplasmas belonging to the elm yellows group and to the stolbur subgroup by PCR amplification of non-ribosomal DNA. Eur. J. Plant Pathol. 103, 507–514. https://doi.org/10.1023/A:1008641411025.
Davosir, D., Šola, I., Ludwig-Müller, J., Šeruga Musić, M., 2023. Flavescence dorée strain-specific impact on phenolic metabolism dynamics in grapevine (*Vitis vinifera*) throughout the development of phytoplasma infection. J. Agric. Food Chem. https://doi.org/10.1021/acs.jafc.3c06501.
Dermastia, M., 2019. Plant hormones in phytoplasma infected plants. Front. Plant Sci. 10, 477. https://doi.org/10.3389/fpls.2019.00477.
Dermastia, M., Škrlj, B., Strah, R., Anžič, B., Tomaž, Š., Križnik, M., Schönhuber, C., Riedle-Bauer, M., Ramšak, Ž., Petek, M., Kladnik, A., Lavrač, N., Gruden, K., Roitsch, T., Brader, G., Pompe-Novak, M., 2021. Differential response of grapevine to infection with '*candidatus* phytoplasma solani' in early and late growing season through complex regulation of mRNA and small RNA transcriptomes. Int. J. Mol. Sci. 22, 3531. https://doi.org/10.3390/ijms22073531.
Ding, Y., Murphy, K.M., Poretsky, E., Mafu, S., Yang, B., Char, S.N., Christensen, S.A., Saldivar, E., Wu, M., Wang, Q., Ji, L., Schmitz, R.J., Kremling, K.A., Buckler, E.S., Shen, Z., Briggs, S.P., Bohlmann, J., Sher, A., Castro-Falcon, G., Hughes, C.C., Huffaker, A., Zerbe, P., Schmelz, E.A., 2019. Multiple genes recruited from hormone pathways partition maize diterpenoid defences. Nat. Plants 5, 1043–1056. https://doi.org/10.1038/s41477-019-0509-6.
Dufour, M.-C., Magnin, N., Dumas, B., Vergnes, S., Corio-Costet, M.-F., 2016. High-throughput gene-expression quantification of grapevine defense responses in the field using microfluidic dynamic arrays. BMC Genom. 17, 957. https://doi.org/10.1186/s12864-016-3304-z.
Eveillard, S., Jollard, C., Labroussaa, F., Khalil, D., Perrin, M., Desqué, D., Salar, P., Razan, F., Hévin, C., Bordenave, L., Foissac, X., Masson, J.E., Malembic-Maher, S., 2016. Contrasting susceptibilities to flavescence dorée in *Vitis vinifera*, rootstocks and wild vitis species. Front. Plant Sci. 7.
Fox, J., 2005. The R Commander: a basic-statistics graphical user interface to R. J. Stat. Soft. 14, 1–42. https://doi.org/10.18637/jss.v014.i09.
Galetto, L., Marzachì, C., Marques, R., Graziano, C., Bosco, D., 2011. Effects of temperature and CO2 on phytoplasma multiplication pattern in vector and plant. Bull. Insectol. 64 (Supplement), S151–S152, 2011 ISSN 1721-8861.
Gambino, G., Boccacci, P., Margaria, P., Palmano, S., Gribaudo, I., 2013. Hydrogen peroxide accumulation and transcriptional changes in grapevines recovered from flavescence dorée disease. Phytopathology® 103, 776–784. https://doi.org/10.1094/PHYTO-11-12-0309-R.
Hoshi, A., Oshima, K., Kakizawa, S., Ishii, Y., Ozeki, J., Hashimoto, M., Komatsu, K., Kagiwada, S., Yamaji, Y., Namba, S., 2009. A unique virulence factor for proliferation and dwarfism in plants identified from a phytopathogenic bacterium. PNAS 106, 6416–6421. https://doi.org/10.1073/pnas.0813038106.
Hren, M., Nikolic, P., Rotter, A., Blejec, A., Terrier, N., Ravnikar, M., Dermastia, M., Gruden, K., 2009a. Bois noir" phytoplasma induces significant reprogramming of the leaf transcriptome in the field grown grapevine. BMC Genom. 10, 460. https://doi.org/10.1186/1471-2164-10-460.
Hren, M., Ravnikar, M., Brzin, J., Ermacora, P., Carraro, L., Bianco, P.A., Casati, P., Borgo, M., Angelini, E., Rotter, A., Gruden, K., 2009b. Induced expression of sucrose synthase and alcohol dehydrogenase I genes in phytoplasma-infected grapevine plants grown in the field. Plant Pathol. 58, 170–180. https://doi.org/10.1111/j.1365-3059.2008.01904.x.
Jülke, S., Ludwig-Müller, J., 2016. Response of Arabidopsis thaliana roots with altered lipid transfer protein (LTP) gene expression to the clubroot disease and salt stress. Plants 5 (2). https://doi.org/10.3390/plants5010002.
Kaldenhoff, R., Grote, K., Zhu, J.J., Zimmermann, U., 1998. Significance of plasmalemma aquaporins for water-transport in *Arabidopsis thaliana*. Plant J 14, 121–128. https://doi.org/10.1046/j.1365-313x.1998.00111.x.
Kaviani, M., Goodwin, P.H., Hunter, D.M., 2022. Differences in gene expression of pear selections showing leaf curling or leaf reddening symptoms due to pear decline phytoplasma. Plants 11, 427. https://doi.org/10.3390/plants11030427.
Laquitaine, L., Gomès, E., François, J., Marchive, C., Pascal, S., Hamdi, S., Atanassova, R., Delrot, S., Coutos-Thévenot, P., 2006. Molecular basis of ergosterol-induced protection of grape against *botrytis cinerea* : induction of type I LTP promoter activity, WRKY, and stilbene synthase gene expression. MPMI 19, 1103–1112. https://doi.org/10.1094/MPMI-19-1103.
Lu, W., Tang, X., Huo, Y., Xu, R., Qi, S., Huang, J., Zheng, C., Wu, C., 2012. Identification and characterization of fructose 1,6-bisphosphate aldolase genes in Arabidopsis reveal a gene family with diverse responses to abiotic stresses. Gene 503, 65–74. https://doi.org/10.1016/j.gene.2012.04.042.
Maixner, M., 2005. Risks posed by the spread and dissemination of grapevine pathogens and their vectors. In: Proceedings of the symposium held at Humboldt University: Introduction and Spread of Invasive Species, pp. 141–146. Berlin.
Malembic-Maher, S., Desqué, D., Khalil, D., Salar, P., Bergey, B., Danet, JL., Duret, S., Dubrana-Ourabah, MP., Beven, L., Ember, I., Acs, Z., Della Bartola, M., Materazzi, A., Filippin, L., Krnjajic, S., Krstić, O., Toševski, I., Lang, F., Jarausch, B., Kölber, M., Jović, J., Angelini, E., Arricau-Bouvery, N., Maixner, M., Foissac, X., 2020. When a Palearctic bacterium meets a Nearctic insect vector: Genetic and ecological insights into the emergence of the grapevine Flavescence dorée epidemics in Europe. PLoS Pathog. 16 (3), e1007967. https://doi.org/10.1371/journal.ppat.1007967.
Mardi, M., Farsad, L.K., Gharechahi, J., Salekdeh, G.H., 2015. In-depth transcriptome sequencing of Mexican lime trees infected with *candidatus* phytoplasma aurantifolia. PLoS one 10, e0130425. https://doi.org/10.1371/journal.pone.0130425.
Margaria, P., Ferrandino, A., Caciagli, P., Kedrina, O., Schubert, A., Palmano, S., 2014. Metabolic and transcript analysis of the flavonoid pathway in diseased and recovered Nebbiolo and Barbera grapevines (*Vitis vinifera* L.) following infection by Flavescence dorée phytoplasma. Plant, Cell Environ. 37, 2183–2200. https://doi.org/10.1111/pce.12332.
Margaria, P., Palmano, S., 2011. Response of the vitis vinifera L. cv. 'nebbiolo' proteome to flavescence dorée phytoplasma infection. Proteomics 11, 212–224. https://doi.org/10.1002/pmic.201000409.
Martins, C., de, P.S., Pedrosa, A.M., Du, D., Gonçalves, L.P., Yu, Q., Jr, F.G.G., Costa, M. G.C., 2015. Genome-wide characterization and expression analysis of major intrinsic proteins during abiotic and biotic stresses in Sweet Orange (*Citrus sinensis* L. Osb.). PLoS one 10, e0138786. https://doi.org/10.1371/journal.pone.0138786.
Miyamoto, K., Enda, I., Okada, T., Sato, Y., Watanabe, K., Sakazawa, T., Yumoto, E., Shibata, K., Asahina, M., Iino, M., Yokota, T., Okada, K., Yamane, H., 2016. Jasmonoyl-L-isoleucine is required for the production of a flavonoid phytoalexin but not diterpenoid phytoalexins in ultraviolet-irradiated rice leaves. Biosci. Biotechnol. Biochem. 80, 1934–1938. https://doi.org/10.1080/09168451.2016.1189319.
Mollayi, S., Zadali, R., Farzaneh, M., Ghassempour, A., 2015. Metabolite profiling of Mexican lime (*Citrus aurantifolia*) leaves during the progression of witches' broom disease. Phytochem. Lett. 13, 290–296. https://doi.org/10.1016/j.phytol.2015.07.010.
Murphy, K.M., Edwards, J., Louie, K.B., Bowen, B.P., Sundaresan, V., Northen, T.R., Zerbe, P., 2021. Bioactive diterpenoids impact the composition of the root-associated microbiome in maize (Zea mays). Sci. Rep. 11, 333. https://doi.org/10.1038/s41598-020-79320-z.
Nawaz, H., Irum, A., Nasim, W., Hussain, N., Usman, M., Alam, J., 2023. Hormonal cross-talk mechanisms and plant immunity or defense: an overview. In: Husen, A., Zhang, W. (Eds.), Hormonal Cross-Talk, Plant Defense and Development. Academic Press, pp. 1–12.
Negro, C., Sabella, E., Nicolì, F., Pierro, R., Materazzi, A., Panattoni, A., Aprile, A., Nutricati, E., Vergine, M., Miceli, A., De Bellis, L., Luvisi, A., 2020. Biochemical changes in leaves of vitis vinifera cv. Sangiovese infected by Bois Noir phytoplasma. Pathogens 9, 269. https://doi.org/10.3390/pathogens9040269.
Nejat, N., Cahill, D.M., Vadamalai, G., Ziemann, M., Rookes, J., Naderali, N., 2015. Transcriptomics-based analysis using RNA-seq of the coconut (*Cocos nucifera*) leaf in response to yellow decline phytoplasma infection. Mol. Genet. Genomics 290, 1899–1910. https://doi.org/10.1007/s00438-015-1046-2.
Pacifico, D., Margaria, P., Galetto, L., Legovich, M., Abbà, S., Veratti, F., Marzachì, C., Palmano, S., 2019. Differential gene expression in two grapevine cultivars recovered from "flavescence dorée. Microbiol. Res. 220, 72–82. https://doi.org/10.1016/j.micres.2018.12.005.
Paolacci, A.R., Catarcione, G., Ederli, L., Zadra, C., Pasqualini, S., Badiani, M., Musetti, R., Santi, S., Ciaffi, M., 2017. Jasmonate-mediated defence responses, unlike salicylate-mediated responses, are involved in the recovery of grapevine from bois noir disease. BMC Plant Biol 17, 118. https://doi.org/10.1186/s12870-017-1069-4.
Pouzoulet, J., Scudiero, E., Schiavon, M., Rolshausen, P., 2017. Xylem vessel diameter affects the compartmentalization of the vascular pathogen *Phaeomoniella chlamydospora* in Grapevine. Front. Plant Sci. 8, 1442. https://doi.org/10.3389/fpls.2017.01442.
Prezelj, N., Covington, E., Roitsch, T., Gruden, K., Fragner, L., Weckwerth, W., Chersicola, M., Vodopivec, M., Dermastia, M., 2016. Metabolic consequences of infection of grapevine (*Vitis vinifera* L.) cv. "Modra frankinja" with flavescence dorée phytoplasma. Front. Plant Sci. 7.
Qiao, K., Huang, W., Li, X., Liang, J., Cai, H., 2023. Combined transcriptomic and metabolomic analyses of defense mechanisms against phytoplasma infection in *Camptotheca acuminata Decne*. Agriculture 13, 1943. https://doi.org/10.3390/agriculture13101943.
R Core Team, 2020. R: a langage and environment for statistical computing. R Foundation for Statistical Computing. Vienna, AustriaURL. https://www.R-project.org/.
Ripamonti, M., Pegoraro, M., Morabito, C., Gribaudo, I., Schubert, A., Bosco, D., Marzachì, C., 2021. Susceptibility to flavescence dorée of different *Vitis vinifera* genotypes from north-western Italy. Plant Pathol 70, 511–520. https://doi.org/10.1111/ppa.13301.
Roggia, C., Caciagli, P., Galetto, L., Pacifico, D., Veratti, F., Bosco, D., Marzachì, C., 2014. Flavescence dorée phytoplasma titre in field-infected Barbera and Nebbiolo grapevines. Plant Pathol 63, 31–41. https://doi.org/10.1111/ppa.12068.
Safi, H., Saibi, W., Alaoui, M.M., Hmyene, A., Masmoudi, K., Hanin, M., Brini, F., 2015. A wheat lipid transfer protein (TdLTP4) promotes tolerance to abiotic and biotic stress in *Arabidopsis thaliana*. Plant Physiol. Biochem. 89, 64–75. https://doi.org/10.1016/j.plaphy.2015.02.008.
Salar, P., Charenton, C., Foissac, X., Malembic-Maher, S., 2013. Multiplication kinetics of flavescence dorée phytoplasma in broad bean. Effect of phytoplasma strain and temperature. Eur. J. Plant Pathol. 135, 371–381. https://doi.org/10.1007/s10658-012-0093-3.

Santi, S., De Marco, F., Polizzotto, R., Grisan, S., Musetti, R., 2013. Recovery from stolbur disease in grapevine involves changes in sugar transport and metabolism. Front. Plant Sci. 4. https://doi.org/10.3389/fpls.2013.00171.

Schmidtmann, E., König, A.-C., Orwat, A., Leister, D., Hartl, M., Finkemeier, I., 2014. Redox regulation of Arabidopsis mitochondrial citrate synthase. Mol. Plant 7, 156–169. https://doi.org/10.1093/mp/sst144.

Schvester, D., Carle, P., moutous, G., 1963. Transmission de la flavescence dorée de la vigne par *Scaphoideus littoralis* ball. Ann. Epiphyt. 14, 175–198.

Tan, Y., Li, Q., Zhao, Y., Wei, H., Wang, J., Baker, C.J., Liu, Q., Wei, W., 2021. Integration of metabolomics and existing omics data reveals new insights into phytoplasma-induced metabolic reprogramming in host plants. PLoS One 16, e0246203. https://doi.org/10.1371/journal.pone.0246203.

Teixeira, A., Martins, V., Frusciante, S., Cruz, T., Noronha, H., Diretto, G., Gerós, H., 2020. Flavescence dorée-derived leaf yellowing in grapevine (*Vitis vinifera* L.) is associated to a general repression of isoprenoid biosynthetic pathways. Front. Plant Sci. 11.

Thévenin, J., Pollet, B., Letarnec, B., Saulnier, L., Gissot, L., Maia-Grondard, A., Lapierre, C., Jouanin, L., 2011. The simultaneous repression of CCR and CAD, two enzymes of the lignin biosynthetic pathway, results in sterility and dwarfism in Arabidopsis thaliana. Mol. Plant 4, 70–82. https://doi.org/10.1093/mp/ssq045.

Trivellone, V., Dietrich, C.H., 2021. Evolutionary diversification in insect vector–Phytoplasma–Plant associations. Ann. Entomol. Soc. Am. 114, 137–150. https://doi.org/10.1093/aesa/saaa048.

Wasternack, C., Feussner, I., 2018. The oxylipin pathways: biochemistry and function. Annu. Rev. Plant Biol. 69, 363–386. https://doi.org/10.1146/annurev-arplant-042817-040440.

Wei, W., Davis, R.E., Nuss, D.L., Zhao, Y., 2013. Phytoplasmal infection derails genetically preprogrammed meristem fate and alters plant architecture. PNAS U S A 110, 19149–19154. https://doi.org/10.1073/pnas.1318489110.

Xue, C., Liu, Z., Dai, L., Bu, J., Liu, M., Zhao, Z., Jiang, Z., Gao, W., Zhao, J., 2018. Changing host photosynthetic, carbohydrate, and energy metabolisms play important roles in phytoplasma infection. Phytopathology® 108, 1067–1077. https://doi.org/10.1094/PHYTO-02-18-0058-R.